
Rotor Faults Diagnosis Using Artificial Neural Networks and Support Vector Machines

Sukhjeet Singh and Navin Kumar

School of Mechanical, Materials and Energy Engineering, Indian Institute of Technology Ropar, Nangal Road, Rupnagar, Punjab, India

(Received 3 June 2013; accepted 1 January 2014)

Unbalance and misalignment are the commonly occurring faults in rotating mechanical systems. These faults are caused mainly due to improper installation or premature failure of the machine components. Detection and diagnosis of faults in rotating machinery is crucial for its optimal performance. In this study artificial neural networks (ANN) and support vector machine (SVM) techniques have been used to determine the effectiveness of statistical features for fault diagnosis in rotating mechanical system using healthy and faulty rotors. The vibration signature responses are obtained and analyzed for healthy shaft without disk (HSWD), healthy shaft with an unbalanced disk (HSWUD), centrally bent shaft without disk (CBSWD) and centrally bent shaft with an unbalanced disk (CB-SWUD) with zero bow phase angle. Their predominant features were fed as input for training and testing ANN and SVM, whereas the relative efficiency of these techniques have been compared for classifying the faults in the test system. The study concludes that these machine learning algorithms can be used for fast and reliable diagnosis of rotor faults.

NOMENCLATURE

| | |
|--------------|---|
| T | Bias or threshold |
| λ_i | Lagrange multipliers |
| $U(\lambda)$ | Lagrange function |
| ϕ_j^h | Bias for hidden layer |
| net_{mn}^h | Net input to hidden layer |
| net_{mk}^o | net input to output layer |
| μ_{mn} | n^{th} input of the m^{th} input vector |
| κ_i | Distance between the margin and the examples μ_i that are lying on the wrong side of the margin |
| ϕ_j^o | Bias for output layer |
| E_m | Sum of squares error |
| O_{mk}^o | Output of output layer |
| V_m | Sum of squares error |
| Δ_m^o | Change in weight w.r.t weight change |
| O_{mj}^h | Output of hidden layer |
| u_{jk}^h | Synaptic weight between hidden and output layer |
| M | Number of iterative step |
| Z_{mk} | Desired output |

1. INTRODUCTION

Rotating machinery diagnostics is an essential function in industrial processes and power generation applications. Failures in a rotating machinery system are quite common and their proper diagnosis depends upon accurate detection of the fault and its location. Most of the faults are caused either because of the incorrect manufacturing practices or because of the extreme operating conditions. These may result in excessive heat generation, looseness and other unwanted wears and tears of the rotating parts causing financial losses. Therefore, a contin-

uous monitoring system is required to detect and diagnose the faults to avoid any such situation.

Faults associated with the rotor-bearing system like unbalanced rotor,^{1,2} bent rotor,³ misaligned rotor,⁴ and rotor rub^{5,6} are discussed in the literature. Many techniques and tools are already in practice for the continuous diagnosis of the various components of the rotating machinery. Li et al.⁷ used the hidden Markov models (HMM) techniques in order to detect various faults namely: rotor unbalance, rotor to stator rub, oil whirl and pedestal looseness in a rotating machinery under speed-up and speed-down conditions. Rolling element bearings defects like outer race, inner race, ball spin and cage faults were discussed by different researchers⁸⁻¹² using different techniques. Also, back-propagation learning algorithm and a multi-layer network have been used to validate the test data for unknown faults.¹³

Fault diagnosis of load machines like gearboxes for common defects like missing tooth and wear of the gear tooth were carried out using wavelet techniques.¹⁴ Kolmogorov-Smirnov test was used by Kar and Mohanty for the detection of faulty gears.¹⁵ The performance of gear fault was detected using ANN and SVM by Samanta.¹⁶ Support vector machines (SVM) were used in the fault diagnosis of machines.¹⁷

The present work deals with the extraction of statistical features from the vibration signatures of a rotor-bearing system and classification of shaft faults using artificial neural network (ANN) and support vector machine (SVM). The flow chart for the shaft health diagnosis is shown in Fig. 1.

A group of statistical features like range, root mean square value, crest factor, kurtosis, skewness and standard deviation have been extracted from time domain. The setup details for simulating the combined unbalance and bent rotor fault in a real experimental machine have been discussed in Section 2.

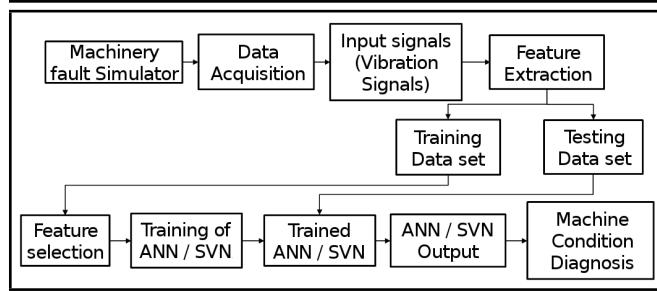


Figure 1. Flow chart of shaft health diagnosis

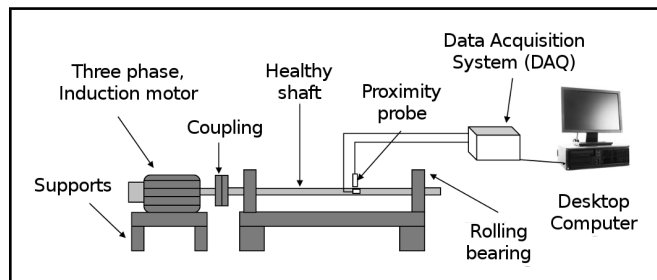


Figure 2. Line diagram of the experimental setup

Section 3 presents the background of the ANN and SVM. The wave forms of the healthy and faulty shaft signals are presented in Section 4. Salient statistical features from the acquired signals were extracted and compiled to form a feature vector which is fed to ANN/SVM for training and testing it is discussed in Section 4. The conclusions are discussed in Section 5.

2. EXPERIMENTAL SETUP AND DATA ACQUISITION

The experimental setup consists of a slotted aluminium disc mounted on a 19.05 mm diameter shaft (cold rolled steel) and the shaft was supported on two identical roller bearings. The schematic of the experimental setup is shown in Fig.2. A three phase 0.75 kW induction motor coupled with a variable frequency drive (VFD) was used for running this arrangement. Reverse dial gauge method was used to align the shaft with the motor end shaft. A pair of proximity probes were mounted radially (in horizontal and vertical directions) with an attachment on the rotor system.

Two shafts, one healthy (HS) and one centrally bent (CBS) with a bend of 200 microns were used to simulate different shaft unbalance conditions. For simulating unbalance, the aluminium disc has threaded holes in which nuts and bolts of pre-determined weight of 17 g could be screwed. The bending natural frequency (ω_n) of the healthy and centrally bent shafts was 59.9 Hz as obtained from the rap test. Data was acquired using a NI 9234 data acquisition card at the sampling rate of 1651 Hz for 1.24 seconds. The numbers of acquired samples were 2048. The system was run from 1.15 Hz to 40.25 Hz with an increment of 1.15 Hz and data was acquired for healthy and faulty shaft conditions. These time-domain data were pre-processed to extract the features which are used as inputs to the classifiers - ANN and SVM techniques.

3. FEATURE EXTRACTION AND SELECTION

The optimal performance of fault diagnosis of a rotating machine depends on appropriate features extraction and features selection techniques. The selection of essential features from the test machine is an important step towards increasing the overall effectiveness of the fault diagnosis process. For analyzing signals and extracting features various techniques are used such as time domain, frequency domain and time-frequency domain.¹⁸

Six statistical features including range, root mean square value, crest factor, kurtosis, skewness and standard deviation were used each for horizontal and vertical response (acquired with a pair of proximity probes) for the healthy and faulty shafts. Then, statistical features of the healthy and the faulty shafts were compiled to form a vector as shown in Table 1 along with speed as an additional feature. A total of 140 instances of experiments were used for the present work. These features are discussed below in detail:

- Range is the difference between the maximum and minimum value of a signal.
- Standard deviation is the measure of dispersion of data sets from its mean. The more spread of data produce higher deviation. Mean and standard deviation can be described as following:

$$x_{mean} = \frac{1}{m} \sum_{i=1}^m x(i);$$

$$x_{std} = \sqrt{\frac{\sum_{i=1}^m (x(i) - x_{mean})^2}{m - 1}}; \quad (1)$$

where $x(i)$ is a signal series for $i = 1, 2, \dots, m$ and m is the number of data points.

- RMS is used to measure the overall power content of the signal. Skewness use the normalized third central moment. Mathematically RMS and skewness can be defined as:

$$x_{rms} = \sqrt{\frac{\sum_{i=1}^m (x(i))^2}{m}};$$

$$x_{skew} = \sqrt{\frac{\sum_{i=1}^m (x(i) - x_{mean})^3}{(m - 1)x_{std}^3}}. \quad (2)$$

- Kurtosis measures the relative peak-edness of the distribution as compared to a normal distribution. Crest factor computes the ratio of the peak level of data over the RMS level. There-fore, the results from the crest factor show the peak of data corresponding to an increase in crest factor value.

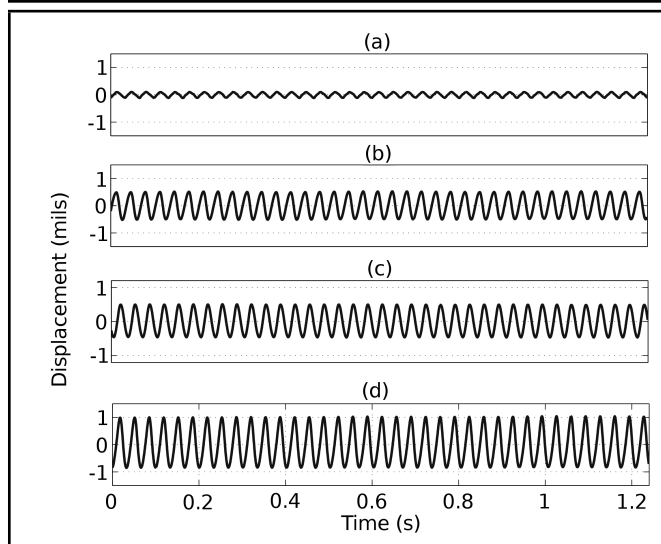


Figure 3. (a, b, c and d) Displacement waveform of the healthy shaft without disk, healthy shaft with unbalanced disk, centrally bent shaft without disk and centrally bent shaft with unbalanced disk with BP of 0° at $\omega_n/2$ respectively

$$x_{kurt} = \sqrt{\frac{\sum_{i=1}^m (x(i) - x_{mean})^4}{(m-1)x_{std}^4}}; \quad (3)$$

$$x_{cf} = \frac{x_{max}}{x_{rms}}$$

The faults which are fully developed or are in incipient stage may not be detected in time domain signals, or could be masked/buried in the noise along with the signals. But, it has already been established by many authors that the fault can be detected using the time domain statistical features even for the shortest duration of the data acquired for the fault.^{10,11,19} The displacement waveforms of the HSWD, HSWUD, CBSWD and CBSWUD with BP of 0° at $\omega_n/2$ are shown in Fig. 3.

3.1. Artificial neural network

Artificial neural network (ANN) is an interconnected network of models based on the biological learning processes of human brain. There are a number of applications of the ANNs in regression analysis, robotics, data analysis, pattern recognition and control. Multi-layer perceptron (MLP) has been used by different researchers in the past for different types of faults and signals taken with the different sensors.²⁰ Essentially, an ANN consists of an interconnected group of artificial neurons. These neurons use a mathematical or computational model for information processing. ANN is an adaptive system that takes its decisions based on information that passes through the network.²¹ The neuronal model as explained in Fig. 4 also includes bias (threshold) which is an external parameter of neural network with constant input.²²

3.2. Back propagation (BP) algorithm

The structure of neurons in a neural network is known as the network architecture. Three different classes of network ar-

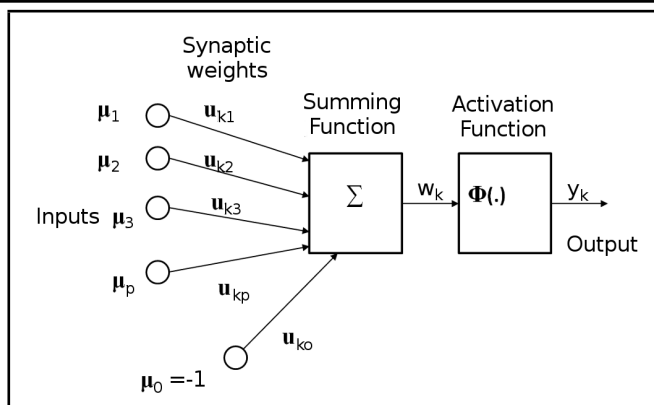


Figure 4. Model of a single non-linear neuron

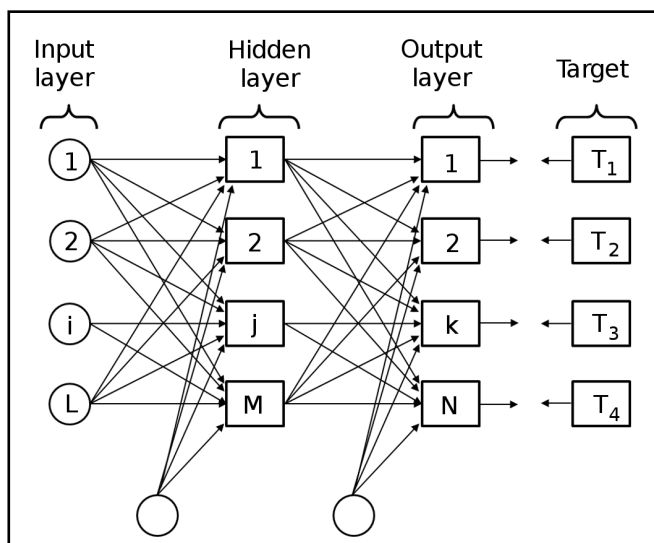


Figure 5. Back propagation algorithm in multi-layer neural network

chitecture are: single layer feed-forward network, multi-layer feed-forward network and recurrent networks. Another important type of neural networks is a multi-layer feed forward network, which is also known as multi-layer perceptrons (MLPs). Back propagation (BP) algorithm is shown in Fig. 5. It consists of two steps which are known as forward pass and backward pass.

3.3. Support vector machine

Support Vector Machines (SVMs) are a new generation learning systems which are based on the statistical learning theory. They belong to the class of supervised learning algorithms in which the learning machine is given a set of inputs with the associated outputs. Cristianini (2000) used SVM for pattern recognition and classification.²³ A simple case of two classes separated by a linear classifier points are shown by triangles and squares in Fig. 6. The plane that separates the two classes is called hyper plane, H . H_1 and H_2 (shown by dashed lines) are the planes that are parallel to plane H and pass through the sample points closest to plane H in these two classes. The planes parallel to H are designated as H_1 and H_2 and they pass through the sample points nearest to H amongst these classes. The distance between the two parallel planes is known as margin. The closest placed data points that are used

Table 1. Sample input vector for ANN/SVM techniques

| Horizontal Proximity Probe Response | | | | | | Vertical Proximity Probe Response | | | | | | | |
|-------------------------------------|-------|--------------|----------|----------|--------------------|-----------------------------------|-------|--------------|----------|----------|--------------------|-----------------|--------|
| Features | | | | | | | | | | | | | Class |
| Range | RMS | Crest Factor | Kurtosis | Skewness | Standard Deviation | Range | RMS | Crest Factor | Kurtosis | Skewness | Standard Deviation | Speed Deviation | |
| 1 | 2 | 3 | 4 | 5 | 6 | 7 | 8 | 9 | 10 | 11 | 12 | 13 | |
| 0.164 | 0.053 | 1.519 | 1.661 | -0.286 | 0.052 | 0.343 | 0.117 | 1.421 | 1.965 | -0.599 | 0.113 | 1.15 | HSWD |
| 0.18 | 0.06 | 1.464 | 1.585 | -0.037 | 0.059 | 0.388 | 0.124 | 1.501 | 1.697 | -0.026 | 0.123 | 2.3 | HSWD |
| 0.105 | 0.036 | 1.621 | 1.643 | -0.401 | 0.035 | 0.29 | 0.097 | 1.607 | 1.466 | -0.029 | 0.096 | 1.15 | HSWUD |
| 0.127 | 0.04 | 1.713 | 1.573 | 0.222 | 0.04 | 0.334 | 0.104 | 1.698 | 1.626 | 0.234 | 0.103 | 2.3 | HSWUD |
| 0.748 | 0.26 | 1.492 | 1.769 | 0.464 | 0.251 | 1.928 | 0.651 | 1.518 | 1.579 | -0.13 | 0.645 | 1.15 | CBSWD |
| 0.79 | 0.278 | 1.475 | 1.545 | 0.193 | 0.277 | 2.035 | 0.707 | 1.458 | 1.561 | 0.152 | 0.705 | 2.3 | CBSWD |
| 0.674 | 0.23 | 1.527 | 1.582 | -0.066 | 0.229 | 1.282 | 0.454 | 1.44 | 1.762 | 0.47 | 0.439 | 1.15 | CBSWUD |
| 0.74 | 0.266 | 1.46 | 1.473 | 0.131 | 0.266 | 1.386 | 0.476 | 1.489 | 1.572 | -0.122 | 0.472 | 2.3 | CBSWUD |

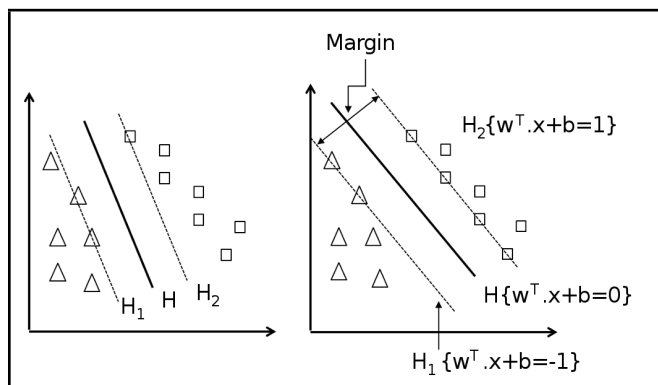


Figure 6. Hyper-plane classifying two classes : (a) small margin (b) large margin

to define the margin are recognized as support vectors or margin of separation.²⁰ The aim of the SVM is to obtain a linear hyper-plane between the H_1 and H_2 hyper-planes so that the margin is maximized.

This problem is solved by reducing it to a convex optimization problem: that is minimizing a quadratic function under linear inequality constraints.²³

4. RESULTS

The displacement waveforms of the HSWD, HSWUD, CBSWD and CBSWUD with BP of 0° at $\omega_n/2$ are shown in Fig. 3. The vibration amplitude of the HSWD is 0.095 mils (r.m.s. value), whereas for HSWUD it is 0.2482 mils (r.m.s. value) at $\omega_n/2$ rotational speed as shown in Figs. 3(a) and 3(b).

Similarly, for the CBSWD CBSWD with an unbalance running at 29.9 Hz with a bow phase angle of 0° , the vibration responses at $(\omega_n/2)$ are 0.4974 and 0.6428 mils (r.m.s. value) respectively. The term bow phase angle at 0° means that the unbalance and the bow are on the same side. So the amplitude of vibration of such a rotor should be higher than that of a healthy rotor running under same conditions.²⁴

An increase in the amplitude of vibration is an indication of a deteriorating shaft condition. Also, the rate of increase of the amplitude is proportional to the degree of defect. It is quite possible to predict the trend of increase in the amplitude of the defective shafts by continuously monitoring the vibration responses. The operator of the machine should be skilled to predict about the type of the fault after looking into the vibration responses. Skilled operators are more difficult to hire

because of their demand for higher salaries. Therefore, it becomes necessary to have an automatic fault diagnostic system which can predict the defect and advise the operator of an appropriate remedy to the problem.²⁵

ANN/SVM training and classification of faults are carried out in WEKA software.²⁶ Training vectors are already compiled and are put as an input. The defects considered in the study are classified using ANN/SVM techniques are as follows: HSWD, HSWUD, CBSWD and CBSWUD zero bow phase angle.

The training vector extracted from the data is shown in Table 1. In Table 2, the magnitudes of the various statistical parameters like range, root mean square value, crest factor, kurtosis, skewness and standard deviation features for every shaft condition have been mentioned at the rotor speed $\omega_n/2$. It is pertinent to mention here that at $\omega_n/2$ speed an increase in the magnitude of statistical variables namely- range, r.m.s., standard deviation and skewness was observed with an increase in the fault condition in comparison to HSWD condition. However, the crest factor and kurtosis variable values show an increase for HSWD condition and they become almost constant for all the remaining shaft conditions at this speed.

The effect of speed on the statistical variables identified for the present study were also studied. It was observed that except for crest factor and kurtosis, all other statistical variables followed a general trend of an increase in the magnitude with an increase of speed as shown in Figs. 7-10.

From the acquired responses, it was analyzed that the amplitude of the vibrations increase with an increase in rotor speed (Fig.3). But it becomes very difficult to differentiate shaft faults individually on the basis of time and frequency domain. Therefore, ANN and SVM techniques were applied to closely related faults for speedy diagnosis on the basis of their statistical features.

These features were fed to WEKA software²⁶ for selecting the appropriate features in order to make decisions using machine learning algorithms. In a multi-class prediction, the results of a test set are often displayed as a two dimensional confusion matrix (Table 3) with a row and column for each class. Each matrix element showed the number of test examples for which the actual class was the row and the predicted class was the column. Results corresponded to large numbers down the main diagonal and small ideally zero; off-diagonal elements

Table 2. Magnitudes of the various statistical features at the rotor speed ($\omega_n/2$)

| | Range | RMS | Crest factor | Kurtosis | Skewness | Standard deviation |
|--------|--------|--------|--------------|----------|----------|--------------------|
| HSWD | 0.2207 | 0.0687 | 1.5235 | 1.6886 | -0.1488 | 0.0687 |
| HSWUD | 1.0431 | 0.357 | 1.4714 | 1.5034 | 0.0164 | 0.3571 |
| CBSWD | 0.9731 | 0.3373 | 1.498 | 1.508 | 0.081 | 0.3374 |
| CBSWUD | 1.893 | 0.6452 | 1.6146 | 1.5684 | 0.2035 | 0.6454 |

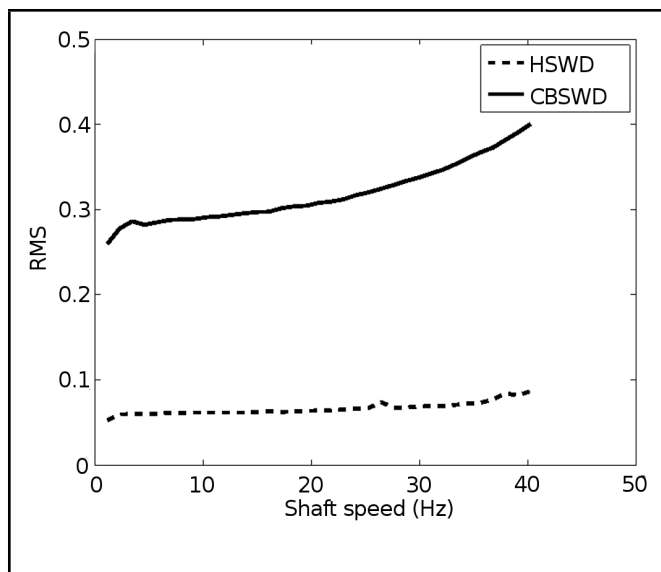


Figure 7. RMS parameter of HSWD and CBSWD at different shaft speeds

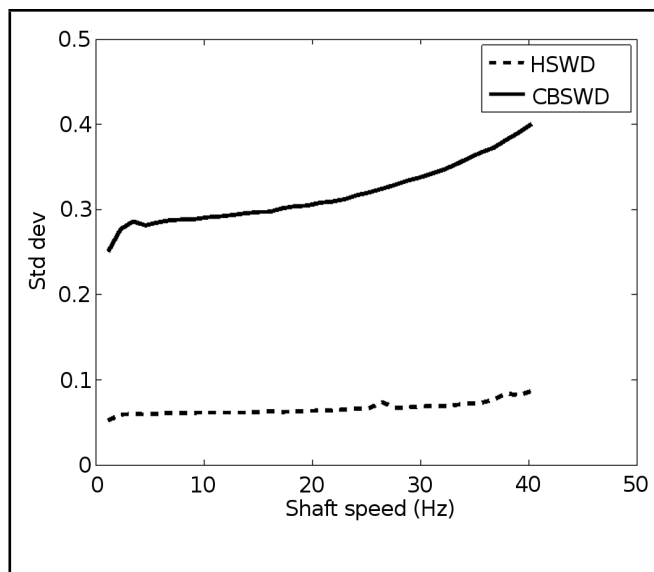


Figure 9. Standard deviation parameter of HSWD and CBSWD at different shaft speeds

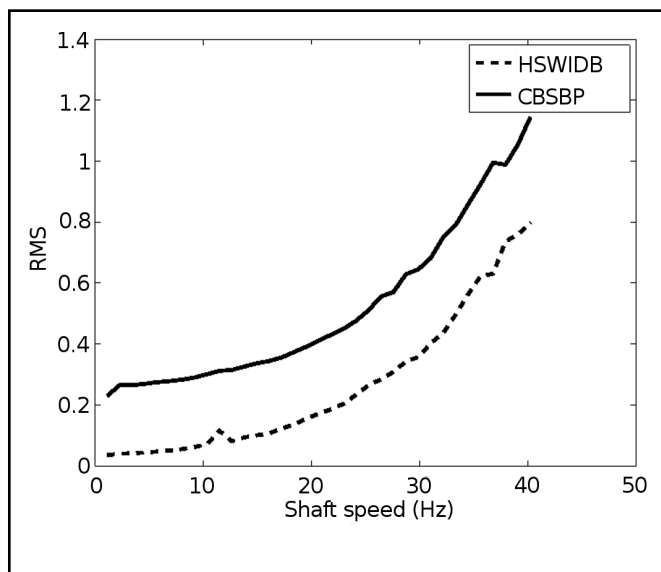


Figure 8. RMS parameter of HSWUD and CBSWUD at different shaft speeds

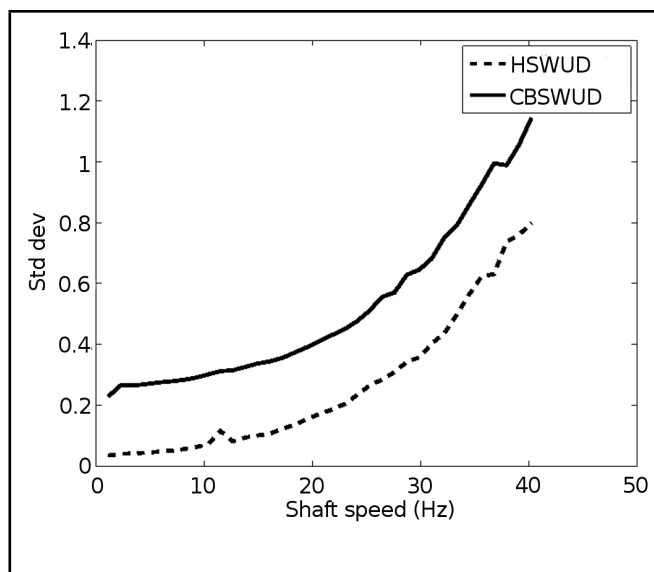


Figure 10. Standard deviation parameter of HSWUD and CBSWUD at different shaft speeds

gave an accurate prediction. After selecting “fault” as an attribute for class, classification was started and the classifier output consisted of the confusion matrix, detailed accuracy by class and evaluation of the success of the numeric prediction.

From Table 3, we inferred that ANN correctly predicted 35, 34, 35 and 35 cases, while SVM classified 35, 34, 35 and 35 cases correctly for HSWD, HSWUD, CBSWD and CBSWUD at zero bow phase angle.

The detailed accuracy of each class has been reported in Table 4. It also gives us the information about TP rate (true positive rate is the number of correctly classified fault divided by the total number of instances for that fault), FP rate (false posi-

tive rate is the number of incorrectly classified fault divided by the total number of instances other than the considered fault), precision, recall and F-measure values for the 4 classes by using ANN and SVM.

The values of various measures of correct classification of faults are tabulated in Table 5. In the present study, the results presented in Table 5 are based on the numeric prediction based on 140 instances and accuracy achieved is 99.2857 % which is better than that of reported by Vyas and Kumar¹³ (90%) and Kankar et al.¹⁹ (95.54 %). Vyas and Kumar’s¹³ results are based on 600 instances for different faults and 100 samples for each fault, whereas Kankar et al.¹⁹ have taken 359 instances

Table 3. Confusion matrix

| HSWD | | HSWUD | | CBSWD | | CBSWUD | | Classified as |
|------|-----|-------|-----|-------|-----|--------|-----|---------------|
| ANN | SVM | ANN | SVM | ANN | SVM | ANN | SVM | |
| 35 | 35 | 0 | 0 | 0 | 0 | 0 | 0 | HSWD |
| 1 | 1 | 34 | 34 | 0 | 0 | 0 | 0 | HSWUD |
| 0 | 0 | 0 | 0 | 35 | 35 | 0 | 0 | CBSWD |
| 0 | 0 | 0 | 0 | 0 | 0 | 35 | 35 | CBSWUD |

Table 4. Detailed accuracy by class

| TP rate | | FP rate | | Precision | | Recall | | Fmeasure | | Class |
|---------|-------|---------|------|-----------|-------|--------|-------|----------|-------|--------|
| ANN | SVM | ANN | SVM | ANN | SVM | ANN | SVM | ANN | SVM | |
| 1 | 1 | 0.01 | 0.01 | 0.972 | 0.972 | 1 | 1 | 0.986 | 0.986 | HSWD |
| 0.971 | 0.971 | 0 | 0 | 1 | 1 | 0.971 | 0.971 | 0.986 | 0.986 | HSWUD |
| 1 | 1 | 0 | 0 | 1 | 1 | 1 | 1 | 1 | 1 | CBSWD |
| 1 | 1 | 0 | 0 | 1 | 1 | 1 | 1 | 1 | 1 | CBSWUD |

Table 5. Evaluation of the success of the numeric prediction

| Parameters | Values (ANN) | | Values (SVM) | |
|----------------------------------|--------------|---------|--------------|---------|
| Correctly classified instances | 139 | 99.2857 | 139 | 99.2857 |
| Incorrectly classified instances | 1 | 0.7143 | 1 | 0.7143 |
| Kappa Statistic | 0.905 | | 0.9905 | |
| Mean absolute error | 0.013 | | 0.2506 | |
| Root mean squared error | 0.0617 | | 0.3128 | |
| Relative absolute error | 3.456 | | 66.7765 | |
| Root relative squared error | 14.2276 | | 72.1726 | |
| Total number of instances | 140 | | 140 | |

for healthy and faulty rotors and bearings. Also, classification accuracy of SVM and ANN is much better than reported by Meyer et al.²⁷

5. CONCLUSIONS

This study presents a potential application of machine learning methods ANNs and SVMs for the fast and reliable detection of shaft faults. Features were extracted from time-domain vibration signals using statistical techniques. The roles of different vibration signals obtained with or without a disc at various speeds have been investigated. The time responses showed that the amplitudes of vibration increase with the addition of different faults. The combined rotor fault that consists of a centrally bent shaft carrying an unbalanced disk at the centre has the high response of the vibrations at almost all the speeds. In total six features have been considered including range, root mean square value, crest factor, kurtosis, skewness and standard deviation features for every shaft condition have been mentioned at the rotor speed $\omega_n/2$. The time taken to run the model by SVM was remarkably less as compared to ANN technique. In our study a healthy and a centrally bent shaft (with zero bow phase angle) have been diagnosed using ANN and SVM at rotor speed $\omega_n/2$ with the success rate as high as 99.2857%. No better results have been reported till date using same conditions at least in the open literature. Present study focuses on the supervised machine learning whereas unsupervised machine learning studies may also be used for detection of rotor faults. Furthermore, this technique can be also used for the diagnosis of multiple fault cases (combination of misalignment, bent rotor and bearing faults). This study presents a potential application of machine learning methods ANNs and SVMs for the fast and reliable detection of shaft faults. Features were extracted from time-domain vibration signals using

statistical techniques. The roles of different vibration signals obtained with or without a disc at various speeds have been investigated. The time responses showed that the amplitudes of vibration increase with the addition of different faults. The combined rotor fault that consists of a centrally bent shaft carrying an unbalanced disk at the centre has the high response of the vibrations at almost all the speeds. In total six features have been considered including range, root mean square value, crest factor, kurtosis, skewness and standard deviation features for every shaft condition have been mentioned at the rotor speed $n/2$. The time taken to run the model by SVM was remarkably less as compared to ANN technique. In our study a healthy and a centrally bent shaft (with zero bow phase angle) have been diagnosed using ANN and SVM at rotor speed $n/2$ with the success rate as high as 99.2857%. No better results have been reported till date using same conditions at least in the open literature. Present study focuses on the supervised machine learning whereas unsupervised machine learning studies may also be used for detection of rotor faults. Furthermore, this technique can be also used for the diagnosis of multiple fault cases (combination of misalignment, bent rotor and bearing faults).

REFERENCES

- Nicholas, J., Gunter, E., and Allaire, P., "Effect of residual shaft bow on unbalance response and balancing of a single mass flexible rotor - 1 Unbalance response," *Journal of Engineering for Power-Transactions of the ASME*, **98**(2), 171–181 (1976).
- Nicholas, J., Gunter, E., and Allaire, P., "Effect of residual shaft bow on unbalance response and balancing of a single mass flexible rotor - 2 Balancing," *Journal of Engineer-*

- ing for *Power-Transactions of the ASME*, **98**(2), 182–189 (1976).
- 3 Edwards, S., Lees, A., and Friswell, M., “The identification of a rotor bend from vibration measurements,” *Society for Experimental Mechanics, Inc, 16th International Modal Analysis Conference* **2**, 1543–1549 (1998).
 - 4 Patel, T. H. and Darpe, A. K., “Experimental investigations on vibration response of misaligned rotors,” *Mechanical Systems and Signal Processing* **23**(7), 2236–2252 (2009).
 - 5 Bachschmid, N., Pennacchi, P., and Vania, A. , “Thermally induced vibrations due to rub in real rotors,” *Journal of Sound and Vibration* **299**(45), 683–719 (2007).
 - 6 Patel, T. H. and Darpe, A. K., “Study of coast-up vibration response for rub detection,” *Mechanism and Machine Theory* **44**(8), 1570–1579 (2009).
 - 7 Zhinong, Li., Zhaotong, Wu., Yongyong, He., and Chu, Fulei., “Hidden Markov model-based fault diagnostics method in speed-up and speed-down process for rotating machinery,” *Mechanical Systems and Signal Processing* **19**(2), 329 – 339 (2005).
 - 8 Samanta, B. and Al-Balushi K. R., “Artificial neural network based fault diagnostics of rolling element bearings using time-domain features,” *Mechanical Systems and Signal Processing* **17**(2), 317–328 (2003).
 - 9 Kar, C. and Mohanty A. R., “Application of Kolmogorov - Smirnov test in ball bearing fault diagnosis,” *Journal of Sound and Vibration* **269**(1-2), 439–454 (2004).
 - 10 Bhavaraju, K. M., Kankar, P. K., Sharma, S. C., and Harsha, S. P., “A comparative study on bearings faults classification by artificial neural networks and self-organizing maps using wavelets,” *International Journal of Engineering Science and Technology* **2**(5), 1001–1008 (2010).
 - 11 Kankar, P. K., Sharma, S. C. and Harsha, S. P. , “Fault diagnosis of ball bearings using continuous wavelet transform,” *Applied Soft Computing* **11**(2), 2300–2312 (2011).
 - 12 Kankar, P. K., Sharma, S. C. and Harsha, S. P., “Fault diagnosis of high speed rolling element bearings due to localized defects using response surface method,” *Journal of Dynamic Systems, Measurement, and Control* **133**(3), 0310071–03100714 (2011).
 - 13 Vyas, N. S. and Satish kumar, D., “Artificial neural network design for fault identification in a rotor-bearing system,” *Mechanism and Machine Theory* **36**(2), 157–175 (2001).
 - 14 Rafiee, J., Rafiee, M. A., and Tse, P. W., “Application of mother wavelet functions for automatic gear and bearing fault diagnosis,” *Expert Systems with Applications* **37**(6), 4568–4579 (2010).
 - 15 Kar, C. and Mohanty A. R., “Multistage gearbox condition monitoring using motor current signature analysis and Kolmogorov - Smirnov test,” *Journal of Sound and Vibration* **290**(1–2), 337–368 (2006).
 - 16 Samanta, B., “Gear fault detection using artificial neural networks and support vector machines with genetic algorithms,” *Mechanical Systems and Signal Processing* **18**(3), 625–644 (2004).
 - 17 Widodo, A. and Yang, B. S. , “Support vector machine in machine condition monitoring and fault diagnosis,” *Mechanical Systems and Signal Processing* **21**, 2560–2574 (2007).
 - 18 Mahamad, A. K. and Hiyama, T., “Development of artificial neural network based fault diagnosis of induction motor bearing,” in *Power and Energy Conference, PECon. IEEE 2nd International*, 1387–1392 (2008).
 - 19 Kankar, P. K., Sharma, S. C. and Harsha, S. P., “Vibration-based fault diagnosis of a rotor bearing system using artificial neural network and support vector machine,” *International Journal of Modelling, Identification and Control* **15**(3), 185–198 (2012).
 - 20 Haykin, S., *Neural Networks: A Comprehensive Foundation*, Prentice Hall PTR, New York, NY, USA (1998).
 - 21 Zurada, J., *Introduction to Artificial Neural Systems*, West St. Paul, Minn. (1992).
 - 22 Kankar, P. K., *Fault diagnosis of rolling element bearings using vibration signature analysis*. PhD thesis, Department of Mechanical and Industrial Engineering, Indian Institute of Technology, Roorkee, India (2011).
 - 23 Cristianini, N. and Shawe-Taylor, J., *An introduction to support vector machines: and other kernel-based learning methods*, Cambridge University Press, New York, NY, USA (2000).
 - 24 Rao, J. S., “A note on Jeffcott warped rotor,” *Mechanism and Machine Theory* **36**(5), 563–575 (2001).
 - 25 Tse, W. P. and Atherton, D. P. , “Prediction of machine deterioration using vibration based fault trends and recurrent neural networks,” *Journal of Vibration and Acoustics* **121**(3), 355–362 (1999).
 - 26 Hall, M., Frank, E., Holmes, G., Pfahringer, B., Reutemann, P., and Witten, I. H., “The WEKA data mining software: an update,” *SIGKDD Explor. Newsl.* **11**(1), 10–18 (2009).
 - 27 Meyer, D., Leisch, F. and Hornik, K. “The support vector machine under test,” *Neurocomputing* **55** (12), 169–186 (2003).